Effects of Water Sorption on the Structure and Properties of Ethylene Ionomers

Shoichi Kutsumizu,*,† Nobuaki Nagao,† Kenji Tadano,‡ Hitoshi Tachino,§ Eisaku Hirasawa,§ and Shinichi Yano†

Department of Chemistry, Faculty of Engineering, Gifu University, Yanagido 1-1, Gifu 501-11, Japan, Gifu College of Medical Technology, Ichihiraga, Seki, Gifu 501-32, Japan, and Technical Center, Du Pont-Mitsui Polychemicals Company, Ltd., Chigusa Kaigan 6, Ichihara, Chiba 299-01, Japan

Received April 13, 1992; Revised Manuscript Received July 23, 1992

ABSTRACT: Effects of water sorption on the structure and properties of poly(ethylene-*co*-methacrylic acid)-based ionomers were investigated by various physicochemical techniques (FTIR, differential scanning calorimetry (DSC), thermogravimetry, X-ray scattering, and dilatometry). It is revealed that water molecules are absorbed preferentially at the COONa ion pairs in both the amorphous and ionic cluster regions, and that three water molecules per one sodium ion form the primary hydration shell. In the more hydrated samples, the excess water molecules are found to locate just around the primary hydration shell. It was found by DSC that both the transition temperature and enthalphy change for the transition near 330 K decrease with increasing hydration. However, this transition was observed even in the fully hydrated samples. These results are well explained by the order–disorder transition model of ionic clusters proposed previously. It is concluded that the ionic clusters consist of the COONa ion pairs and a small portion of the polyethylene backbones.

Introduction

Ionomers are generally defined as linear polymers with predominantly nonpolar backbones which contain 10 mol % or less ionic moieties within the backbones or as side groups. The hydrophilic ionic moieties tend to separate from the hydrophobic polymer matrix, and frequently condense to form ionic aggregates, which are termed ionic multiplets or ionic clusters according to the first theoretical model presented by Eisenberg.[1] The formation of ionic aggregates, which act as physical cross-links, gives drastic changes in polymer properties such as the bending modulus, tensile strength, impact resistance, and melt viscosity.[2-5] Moreover, the ionic aggregation sometimes produces new functional properties such as ionic transport[6] and O_2 molecule sorption.[7,8] Therefore, to date, various ionomers have been developed and extensively studied to clarify the formation and structure of ionic aggregates. The convincing structure of ionic aggregates, however, still remains unanswered because of their colloidal size (20–100 Å). In this paper, the term "ionic cluster" is used in a broad sense.

Generally, poly(ethylene-*co*-methacrylic acid) (EMAA)-based ionomers consist of three regions, as Longworth and co-workers[9] pointed out: a crystalline region of the polyethylene part of the chains, an amorphous region including isolated groups such as COOH and metal carboxylates, and an ionic cluster region. In the X-ray scattering profile, therefore, two peaks are generally observed; the "ionic" peak seen in the small-angle region, arising from ionic clusters, and a peak near $2\theta = 20°$ assigned to (110) and (200) diffractions from the polyethylene crystalline region. A broad halo from the amorphous region is superposed on the latter peak.

The EMAA-based ionomers exhibit a first-order transition near 330 K (T_i) below the melting point of the crystalline region (T_m), and this transition undergoes a characteristic thermal hysteresis. From the differential scanning calorimetric (DSC),[10,11] dilatometric,[10,11] dielectric,[12,13] mechanical[14,15] and far-infrared spectral[16] results, we interpreted this transition as an order–disorder transition within the ionic cluster.[10,11] The ionic clusters are in an ordered state at room temperature, and act as rigid cross-links (strong associations). Above T_i, the ordered structure is transformed into a disordered one, which acts as a loose cross-link (weak association). When the sample is cooled to room temperature from a temperature above T_i, the ionic clusters are still in the disordered state, but gradually reconstruct the ordered structure; the ionic clusters revert to the original ordered state with a long relaxation time (about 40 days at room temperature), because the salt groups "drag" the hydrocarbon chains. We have demonstrated that this model can well explain the various physical properties of ethylene ionomers[14,15,17-19] although it has not been proven with direct evidence yet.

It is well known that moisture absorption largely affects the physical properties of polymer systems. Effects of water sorption on EMAA-based ionomers have been studied by various techniques such as X-ray scattering,[9,20-23] dielectric[24] and mechanical[9] measurements, Fourier transform infrared (FTIR) spectroscopy,[25,26] and gravimetric sorption measurements:[27] Longworth et al.[9,21] first pointed out that a small amount of water sharpened and intensified the ionic peak in the small-angle X-ray scattering (SAXS) region, and that saturation with water reduced it. Cooper et al.[20] and MacKnight et al.[22] also obtained SAXS results similar to those by Longworth et al. On the other hand, dielectric and mechanical measurements showed a plasticizing effect of water. Coleman et al.[25] pointed out that the slow absorption of water caused broadening of the carboxylate asymmetric stretching band during annealing studies which had been considered by the same researchers[28] to be due to the formation of ionic clusters. All these results have demonstrated that water sorption obviously influences the structure and properties of EMAA-based ionomers because sorbed water preferentially affects the ionic cluster region.

In this investigation, we are interested in the water sorption effect on the structure and properties of EMAA-

† Gifu University.
‡ Gifu College of Medical Technology.
§ Du Pont-Mitsui Polychemicals Co. Ltd.

0024-9297/92/2225-6829$03.00/0

based ionomers. Samples used here are 60% and 90% neutralized sodium salts of EMAA where well-formed ionic clusters have been confirmed by several physical techniques. To examine the water sorption behavior, we used FTIR spectroscopy, DSC, thermogravimetry (TG), X-ray scattering, and dilatometry. The mechanism of water sorption is discussed, and it is indicated that changes in physical properties by water sorption can be explained by the order–disorder transition model of ionic clusters mentioned above.

Experimental Section

Materials. EMAA is ACR-1560 of Du Pont-Mitsui Polychemicals Co. Ltd., whose MAA content is 5.4 mol %. Neutralization with sodium cation was accomplished by a melt reaction of EMAA with Na_2CO_3 in an extruder at 450–530 K.[15] Pellet samples obtained were reformed into sheets by compression molding at about 430 K, and stored at room temperature in a vacuum desiccator for more than 40 days. In this paper, we define the above samples as dry samples, although they still contain 0.2–0.4 wt % water (residual water).

Measurements. To obtain water-sorbed samples, the dry samples were kept in a desiccator at about 300 K under several relative humidity conditions, which were produced by saturated aqueous solutions of appropriate salts. The weight gain due to water sorption was measured in an open state by using a Mettler AE163 balance with a sensitivity of 10^{-5} g. The residual water in the dry samples was determined from the weight loss by vacuum-drying at about 450 K for 40 min, where no conversion to the carboxylic anhydride was confirmed by IR spectra (no new bands at 1735, 1780 and 1764, 1802 cm^{-1} were observed[29]). Hereafter, we denote the samples as EMAA–xNa–$y$$H_2O$, where x is the degree of neutralization by sodium and y is the H_2O/COONa molar ratio including the residual water.

Two types of experiments were undertaken to study the effect of water sorption on the physical properties: The thin films ca. 0.05 mm thick were used for IR spectroscopic measurements, where equilibrium water sorption was achieved within 24 h. For DSC, TG/DTA (differential thermal analysis), X-ray scattering, and dilatometric measurements, the sheets of ca. 0.5-mm thickness were used; the sheets were exposed to moisture for about 10–20 days prior to the measurements. The weight change of the sheets indicated that it required more than 1 month to obtain the complete equilibrium.

DSC measurements were carried out with a Seiko Denshi SSC-5000 differential scanning calorimeter at heating/cooling rates of 10 K/min. The instrument was calibrated by indium (mp 156.6 °C, ΔH = 28.45 cal/g) and tin (mp 231.9 °C, ΔH = 59.5 cal/g). Samples of 10–20 mg were weighed to 10^{-2} mg, and placed in aluminum sample pans without sealing.

Thermal gravimetric analysis was carried out with a Seiko Denshi TG-DTA system at a heating rate of 10 K/min under a dry N_2 flow of ca. 200 mL/min.

The IR spectra were measured with a Perkin-Elmer 1640 FTIR spectrometer at room temperature. Each trace represents the average of 64 scans at 4-cm^{-1} resolution. Spectra at elevated temperatures were obtained by using an OMRON HT-32 high-temperature cell equipped with an OMRON E5T controller, where each trace represents the average of 16 scans.

X-ray scattering measurements were performed with a Mac Science X-ray generator (MXP^3 system) operated with a copper target at a 50-kV accelerating potential and 40-mA emmision current. The Cu $K\alpha$ radiation (λ = 1.540 50 Å) was selected with a graphite monochromator. The divergence and scattering slits were 0.5°, and the receiving slit was 0.15 mm. Samples were scanned in air at 1.0 deg/min.

Thermal expansions were measured at heating/cooling rates of ca. 0.5 K/min using a glass capillary dilatometer (0.6-mm i.d.), in which the samples were carefully immersed in liquid mercury in vacuo to avoid a formation of voids on the surface of the sample. The volume change of the samples with temperature was calculated from the readings of the height of mercury in the capillary of the dilatometer. The density, d, at 298 K was obtained by a buoyancy method with benzene.

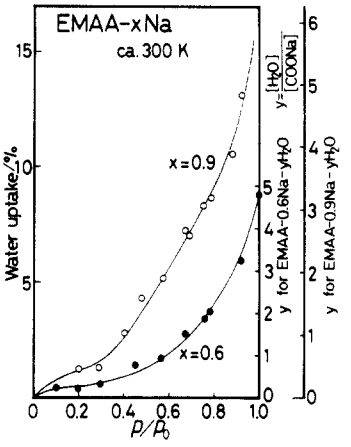

Figure 1. Sorption isotherms of water molecules for EMAA–0.9Na and –0.6Na at 300 K.

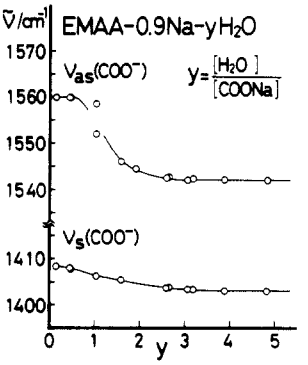

Figure 2. Peak maxima of the carboxylate asymmetric and symmetric stretching bands versus the H_2O/COONa molar ratio (y) for EMAA–0.9Na–$y$$H_2O$.

Results and Discussion

Sorption Isotherms. Figure 1 shows the sorption isotherms of water molecules for EMAA–0.9Na and –0.6Na. Isotherms of the two samples exhibit similar sigmoidal sorption curves. These results are very consistent with those reported by Tsujita et al.[27] At low relative humidities ($p/p_0 < 0.3$), Langmuir-type sorption occurs, where COONa groups both in the amorphous region and in the surface of the ionic clusters may be considered as the Langmuir sorption sites. When the relative humidity (p/p_0) is increased to about 0.3, a solution-type sorption begins to occur. This suggests that water molecules begin to be incorporated into the inside of the ionic clusters in this humidity region.

IR Spectra. Figure 2 shows plots of peak maxima of the carboxylate asymmetric ($\nu_{as}(COO^-)$) and symmetric ($\nu_s(COO^-)$) stretching bands versus water content (y) for EMAA–0.9Na. Below y = 0.5, hydration seems not to affect the peak maxima of the $\nu_{as}(COO^-)$ and $\nu_s(COO^-)$. They locate at 1560 and 1408 cm^{-1}, respectively. When y is larger than 0.5, the water sorption behavior changes from the Langmuir-type water sorption to that of the solution type (Figure 1), and the $\nu_{as}(COO^-)$ gradually shifts to lower frequencies and is leveled off at 1542 cm^{-1} around y = 3. The $\nu_s(COO^-)$ also shifts from 1408 cm^{-1} (y = 0.5) to 1403 cm^{-1} (y = 3). Both bands show no further shift above y = 3. The solid state of sodium *n*-hexanoate exhibits $\nu_{as}(COO^-)$ and $\nu_s(COO^-)$ at 1560.6 and 1415.9 cm^{-1}, respectively, and its aqueous solution exhibits them at 1544.8 and 1408.3 cm^{-1}, respectively.[30] The difference in the peak frequency of $\nu_{as}(COO^-)$ between the two states

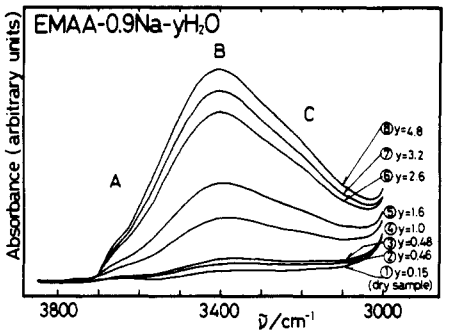

Figure 3. OH stretching region of water molecules in the IR spectra of EMAA–0.9Na–yH$_2$O with various water contents.

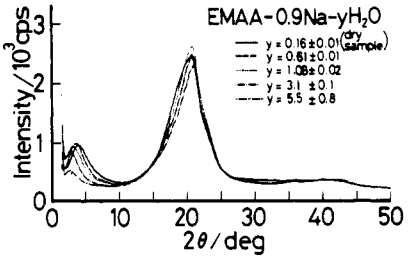

Figure 4. Effect of water sorption on the X-ray scattering pattern of EMAA–0.9Na. The y = 0.61 curve in the region above 2θ = 10° is omitted for clarity.

of sodium n-hexanoate seems to correspond well with that on hydration for EMAA–0.9Na as described above. Therefore, the observed change suggests that three water molecules hydrate with one COONa ion pair in EMAA–0.9Na to form a primary hydration shell, and that the excess of sorbed water molecules exists just outside the primary hydration shell.

Similar results were reported by Lowry and Mauritz[31] for perfluorosulfonate ionomers (Nafion); the $\nu_s(SO_3^-)$ peak shifted to the lower frequency side and sharpened as the water content increased. They explained these changes by the decrease of interaction between the SO_3^- anion and countercation by the shielding effect of the hydrated water molecules. They also proposed a four-state model to explain the hydration–dissociation equilibrium of Nafion ionomers with increasing water content as follows: (1) Ion pairs are surrounded by water molecules, but the anion–cation interaction is virtually not disturbed. (2) The anion–cation interaction is somewhat distrubed by surrounding water molecules. (3) Each anion and cation form a primary hydration shell and contact each other. (4) The hydrated ion pairs are completely dissociated. In EMAA-based ionomers, our observation also indicates that the ionicity of the COO–Na bond increases in the same manner with the increase of hydration. However, the number of water molecules that form the primary hydration shell in EMAA–0.9Na is 3 and smaller than the usual coordination number of 4 for the hydrated sodium ion.[32] This implies that the COONa ion pairs do not completely dissociate. Even fully hydrated ion pairs in EMAA–0.9Na may remain in a state similar to the second hydration–dissociation state in Nafion described above. This difference in the hydration behavior between EMAA-based ionomers and Nafion seems to originate in the difference of acidity between COOH and SO_3H groups.

Figure 3 shows the OH stretching region of water molecules in the IR spectra of hydrated EMAA–0.9Na. On the basis of the assignments for a hydrated Nafion by Falk,[33] three bands marked A, B, and C in Figure 3 can be assigned as follows: The main band around 3400 cm^{-1}, labeled B, is associated with the OH groups of sorbed water molecules that form hydrogen bonds. The frequency is lower than that of liquid water (ca. 3490 cm^{-1}).[34] However, no spectroscopic distinction is observed for two possible types of hydrogen bonding, water···water and water···carboxylate. The smaller band near 3650 cm^{-1} labeled A is considered to originate in the OH groups of nearly free water molecules, which are isolated in the amorphous region and free from hydrogen bonds. This frequency is close to that of gas-phase water (ν_1 = 3657 cm^{-1}; ν_3 = 3756 cm^{-1}). The band C around 3200 cm^{-1} seen as a shoulder may be assigned to the overtone $2\nu_2$ of the HOH bending vibration which couples with the lower-frequency OH stretching mode, ν_1, through the Fermi resonance interaction.

In Figure 3, the frequency of band B gradually increases from ca. 3350 cm^{-1} (y = 0.16) to a constant value of ca. 3400 cm^{-1} around y = 3 with increasing hydration. This result reminds us of the fact that the frequency shift of $\nu_{as}(COO^-)$ stopped around y = 3 as seen in Figure 2.

Although we could not exactly determine the individual areas of bands A and B because of their severe overlapping, the area ratio of band A to B at y = 4.8 was roughly estimated to be on the order of 1/40. Here, we neglect the contribution of band C because of its very weak intensity. This ratio does not directly reflect the number ratio of free water molecules to hydrogen-bonded water molecules, because the IR absorptivity of OH vibrations is enhanced with hydrogen bonding.[35] Nevertheless, the overwhelming intensity of band B compared with that of band A indicates that most of the sorbed water molecules, including water molecules outside the primary hydration shell of the COONa ion pair, are strongly hydrogen-bonded and give rise to band B. Tsujita et al.[36] also pointed out from the cluster function analysis that the formation of a water cluster occurs at high relative humidities in a sodium salt of poly(styrene-*co*-methacrylic acid). These results contrast with those in Nafion,[33] in which sorbed water moelcules are more weakly hydrogen-bonded than liquid water.

IR spectra in the 700–760-cm^{-1} region give us information on the effects of water sorption on the crystalline region. The dry sample of EMAA–0.9Na exhibited two bands, one at 720 cm^{-1} and the other at 730 cm^{-1} seen as a shoulder. Both bands can be assigned to the CH_2 rocking motion, and the splitting is due to the presence of polyethylene crystallites. As might be expected, this splitting and the absorbance of the 720-cm^{-1} band did not change with the hydration up to y = 4.8 due to no water absorptibity of polyethylene crystallites.

X-ray Scattering. More direct information on the structure of ionic clusters and polyethylene crystallites in the ethylene ionomer can be obtained from the X-ray scattering. Figure 4 shows the effects of water sorption on the X-ray scattering pattern of EMAA–0.9Na. Variation of the y values means a change of the water content during the measurement. All five patterns exhibit two peaks: A peak in the 2θ range of 2.5–4°, corresponding to a Bragg spacing of 23–32 Å, is clearly assigned to the ionic peak. The other peak near 20° is the "polyethylene" peak that comes from both the amorphous and polyethylene crystalline regions. Clearly, the polyethylene peak is insensitive to hydration until y = 3.1, and further hydration (y = 5.5) slightly decreases the lower-angle side of the peak.

As y increases, the ionic peak moves toward smaller 2θ, i.e., larger Bragg spacings, but its intensity is almost unchanged until y = 3.1. At y = 5.5, this peak still remains, but is obviously smaller compared with that of y = 3.1.

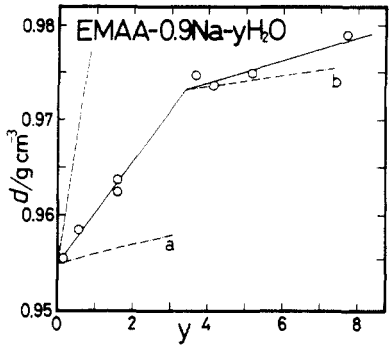

Figure 5. Density (d) at 298 K versus water content (y) for EMAA–0.9Na–yH$_2$O. The dashed curve and dashed-and-dotted, a and b, curves are the ones calculated with eqs 1–3 in the text, respectively.

These observations agree with those by Longworth and co-workers.[9,21] In Nafion[37,38] and sulfonated polystyrene-based ionomers,[39] water sorption shifts their ionic peaks to the lower-angle side and intensifies them. Intensifying the ionic peak due to water sorption is contrary to our results in EMAA–0.9Na. This can be explained by the difference in the acidity between SO_3H and COOH groups. In fact, in Nafion and sulfonated polystyrene-based ionomers, it has been pointed out that the average number of ionic groups in each ionic cluster increases with hydration as a result of an increase in ionicity of the anion–cation bond.[37-39] In the EMAA–0.9Na ionomer, since this tendency is scarcely seen, both the number of ionic clusters and the number of ionic groups per ionic cluster seem to be almost unchanged with hydration. This interpretation is supported by the IR results (Figure 2), which indicate that the COONa ion pairs scarcely dissociate by hydration (i.e., in water) as compared with the SO_3Na ion pairs.

Although the Bragg spacing of the ionic peak does not express the averaged size of the ionic clusters on the basis of either the core–shell model[22] or the liquid-like model,[40] its shift to the lower-angle side certainly means an increase of the size of the ionic clusters. Hence, the shift observed suggests a swelling of the ionic clusters by hydration, because both the number of the ionic clusters in the sample and the number of the COONa ion pairs per ionic cluster may be unchanged by hydration as already pointed out. Generally the scattering intensity is closely connected with two factors: the number of ionic clusters per unit volume and the electron density difference between the amorphous and ionic cluster regions. Since the former factor seems to be scarcely unchanged by hydration in EMAA-based ionomers, the decrease in intensity of the ionic peak by hydration may originate in the decrease of the electron density difference between the ionic cluster and surrounding amorphous regions by hydration. Therefore, the excess of water molecules for the fully hydrated sample (y = 5.5) may be absorbed in the vicinity of the ionic clusters.

Dilatometry. Figure 5 shows plots of the density, d, at 298 K versus the water content (y) for EMAA–0.9Na. When y increases, the value of d rapidly increases below y = 3.4, and above y = 3.4 it increases slowly. It should be noted that the d versus y curve bends near y = 3.4, at which the shift of the $\nu_{as}(COO^-)$ band by hydration is depressed as shown in Figure 2.

Provided that the water molecules are absorbed in some voids of either the amorphous or ionic cluster regions without swelling of the sample, the increase in d by water sorption is expressed as

$$d = 0.9548(1 + 0.054 \times 0.9 \times 18.015y/32.26) \quad (1)$$

where 32.26 is the "unit weight" of $(C_2H_4)_{0.946}(CH_2C(CH_3)COONa_{0.9}H_{0.1})_{0.054}$, and 0.9548 is the density (g/cm^3) of the completely dry sample, obtained by extrapolation of the least-squares fit of the measured points to y = 0. The calculated curve from eq 1 gives the dashed line in Figure 5. If the water molecules are absorbed as liquid water, d can be calculated as

$$d = \frac{32.26 + 0.054 \times 0.9 \times 18.015y}{32.26/0.9548 + 0.054 \times 0.9 \times 18.068y} = \frac{32.26 + 0.8755y}{33.786 + 0.8781y} \quad (2)$$

(the dashed-and-dotted line, a, in Figure 5, where 18.068 is the molar volume (cm^3/mol) of liquid water at 298 K. In the lower hydration region below y = 3.4, the observed curve lies between the above two calculated curves. In the higher hydration region above y = 3.4, if the excess of water molecules beyond y = 3.4 behaves as liquid water, d is given by

$$d = \frac{32.26 + 0.8755y}{36.209 + 0.8781(y - 3.4)} \quad (3)$$

and is shown as the dashed-and-dotted line, b, in Figure 5, which well explains the observed curve above y = 3.4. Therefore, these data support that water molecules of less than three per COONa are absorbed at the COONa ion pairs in both the amorphous and ionic cluster regions to form the primary hydration shell, and that the excess of water molecules are absorbed in the vicinity of the ionic clusters and behave as liquid water.

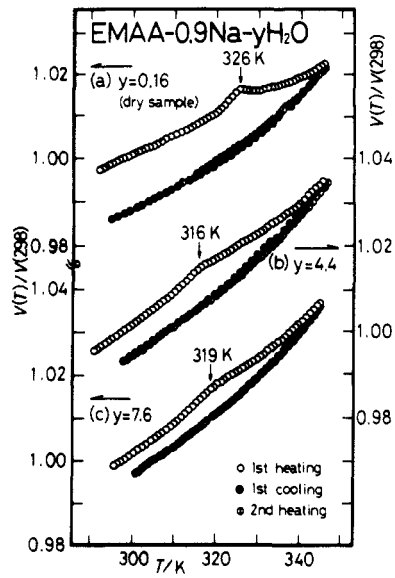

Figure 6. Normalized specific volume ($V(T)/V(298)$) versus temperature for EMAA–0.9Na–yH$_2$O at 3 degrees of hydration in the temperature range from room temperature to 345 K.

Figure 6 shows plots of the normalized specific volume (where specific volume, V, is the reciprocal of d) versus temperature for EMAA–0.9Na at three degrees of hydration. Each thermal cycle was performed in the temperature range between room temperature and 345 K below T_m. The dry sample shows one peak near 326 K (T_i) in the first heating, but it is depressed in the first cooling and second heating. In the first cooling, the value of V at room temperature is smaller than that of the original sample, and the V versus temperature curve for the second heating is almost the same as that for the first cooling. We explained this characteristic thermal hysteresis of the V

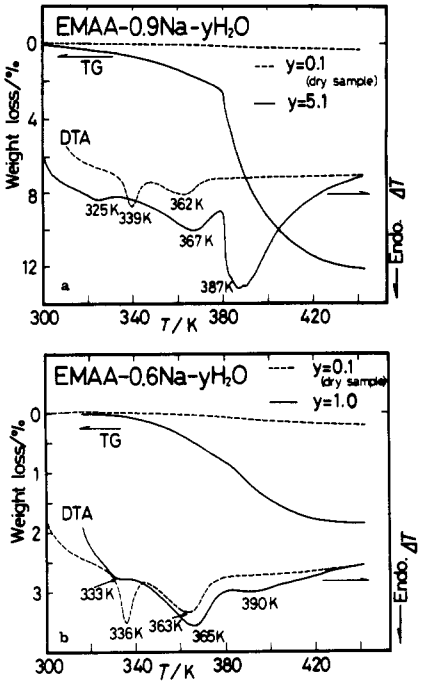

Figure 7. TG and DTA thermograms for a dry and hydrated sample of (a) EMAA–0.9Na and (b) EMAA–0.6Na.

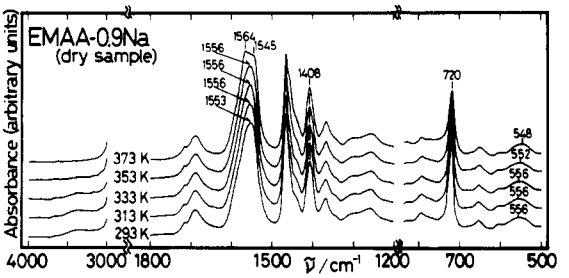

Figure 8. Temperature dependence of the IR spectra in the ranges of 4000–2000, 1800–1200, and 800–500 cm^{-1} for dry EMAA–0.9Na.

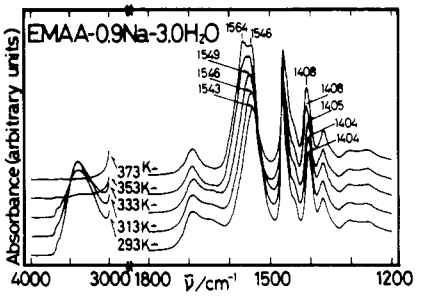

Figure 9. Temperature dependence of the IR spectra in the ranges of 4000–2000 and 1800–1200 cm^{-1} for EMAA–0.9Na–3.0H_2O.

versus temperature curves by proposing the order–disorder transition model of the ionic clusters[10,11] outlined in the Introduction.

When the degree of hydration increases, the peak of V at T_i is depressed and shifts to lower temperatures. At the same time, the decrease of V at room temperature by the thermal cycle, ΔV, becomes smaller with increasing hydration. These results can also be explained by the order–disorder transition model; the sorbed water molecules hydrate the ion pairs inside the ionic clusters and more or less destroy the ordered structure in the ionic clusters. However, the fully hydrated sample still maintains a small peak of V and therefore a small amount of ΔV. This result suggests that some structural order exists even in the fully hydrated ionic clusters at room temperature.

TG/DTA Data. The TG and DTA thermograms for both dry and hydrated samples of EMAA–0.9Na are illustrated in Figure 7a, where the solid curves are for the hydrated sample (y = 5.1) and the dashed ones are for the dry sample (y = 0.1).

The DTA thermogram shows that the dry sample has two endothermic peaks near 339 and 362 K, which correspond, in our model, to T_i and T_m, respectively. The hydrated sample shows another endothermic peak at 387 K in addition to the above two peaks. The TG thermogram clearly indicates that this new peak comes from the release of sorbed water; very gradual loss of about 2.5% of the original weight (about 20% of sorbed water) is seen from 300 to 380 K, and rapid weight loss occurs above 380 K. The peak at 367 K (T_m) in the hydrated EMAA–0.9Na is about twice as large as the peak at 362 K (T_m) in the dry sample. This may be caused by superposition of the water loss below 387 K.

With increasing water content, the transition at T_i moves from 339 to 325 K, and is depressed. The observed trend was also seen in DSC measurements (Figure 10). The TG and DTA thermograms of a dry and hydrated EMAA–0.6Na was also studied and shown in Figure 7b. The results are essentially the same as obtained in EMAA–0.9Na.

Temperature Dependence of IR Spectra. Figure 8 shows the temperature dependence of the IR spectra for a dry EMAA–0.9Na in the ranges of 4000–2000, 1800–1200, and 800–500 cm^{-1}.

The carboxylate asymmetric stretching band ($\nu_{as}(COO^-)$) is observed as a peak at ca. 1555 cm^{-1} between 293 and 353 K, but splits into two bands at 1564 and 1545 cm^{-1} at 373 K above T_m. This splitting is also reported by Coleman et al.;[25,28] they concluded that the loss of residual water causes this splitting and that the splitting itself is essentially due to a demand of symmetry. On the other hand, the carboxylate symmetric band ($\nu_s(COO^-)$) is observed at 1408 cm^{-1}, independent of temperature. In the lower-frequency region below 1000 cm^{-1}, the band attributable to the C–C–C wagging mode[41] is observed at 556 cm^{-1} at 293 K. Upon heating, this band scarcely changes below 333 K, but shifts to lower frequencies above 333 K (e.g., 552 cm^{-1} at 353 K and 548 cm^{-1} at 373 K). This suggests that softening of the polymer backbone occurs near T_i of our model.

The temperature dependence of the IR spectra for EMAA–0.9Na–3.0H_2O is shown in Figure 9. The OH stretching bands around 3400 cm^{-1} and the HOH bending bands about 1650 cm^{-1} are observed between 293 and 333 K, but completely disappear at 373 K above T_m. This should be caused by the loss of water molecules. In fact, the water content (y) decreased from 3.0 to 0.48 during this IR measurement from 293 to 373 K.

The $\nu_{as}(COO^-)$ band gradually shifts from 1543 cm^{-1} at 293 K to 1549 cm^{-1} at 333 K, and begins to split into two bands at 353 K above T_i; they reach 1564 and 1546 cm^{-1} at 373 K above T_m. In connection with this, the $\nu_s(COO^-)$ band seen around 1404 cm^{-1} between 293 and 333 K suddenly shifts to 1408 cm^{-1} at 353 K. Clearly, these results indicate the loss of the sorbed water molecules. Therefore, it may be concluded that the transition at T_i in the hydrated samples accompanies the desorption of the water molecules absorbed at/in the COONa ion pairs.

DSC Data. Figure 10shows the effect of water uptake on the DSC thermogram of EMAA–0.9Na, where the DSC curves show the first heating process up to 453 K; the final sample weight indicated that all of the water contained

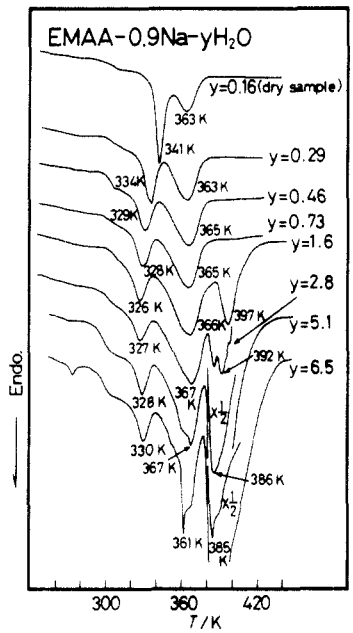

Figure 10. Effect of water uptake on the DSC thermogram of EMAA–0.9Na.

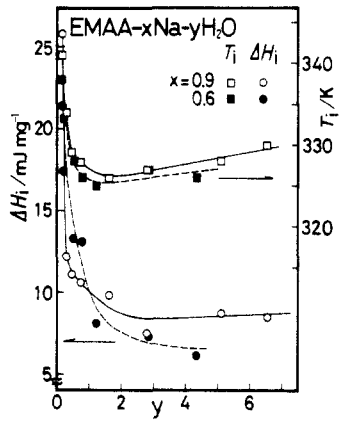

Figure 11. T_i and ΔH_i versus the water content (y) for EMAA–0.9Na and –0.6Na.

at room temperature was lost during the measurement, changing the sample to the dry one.

In the dry sample ($y = 0.16$), two endothermic peaks are observed at 341 and 363 K, which are, in our model, assigned to the order–disorder transition of ionic clusters (T_i) and the melting of the polyethylene crystalline region (T_m), respectively. As the water content (y) increases, the values of T_i and ΔH_i decrease, but in the water content larger than $y = 3$, they show almost constant values. On the other hand, the values of T_m and ΔH_m slightly increase with increasing y. Moreover, a new endothermic peak, clearly caused by the loss of the sorbed water (see Figure 7a), is observed near 390 K above $y = 1.6$.

Figure 11 summarizes the variation of T_i and ΔH_i with the water content (y) for EMAA–0.9Na and –0.6Na. In this case, each ΔH_i is calculated as the enthalpy change per unit weight of the dry sample. From Figures 10 and 11, several features are noted here in connection with the order–disorder transition model of ionic clusters.

First, only the lower-temperature transition at T_i was largely affected by water sorption. This suggests that the lower-temperature transition is certainly associated with the ionic cluster region and not with the polyethylene chains. Because this transition exists regardless of the presence of water in the sample, the lower-temperature peak can be said not to be due to a chemical volatilization associated with the residual water but to a physical structural transition. Therefore, the water sorption effect of T_i provides clear evidence that supports our model of assigning T_i to the order–disorder transition in the ionic clusters.[10,11]

Second, the value of ΔH_i rapidly decreased with the water content. This indicates that the water molecules are incorporated into the ionic clusters and destroy some of their structural order. It is considered that the destruction of the structural order inside of the ionic clusters weakens the strength of cross-linking of the polymer backbone and lowers T_i.

Third, the fully hydrated samples of both EMAA–0.9Na and –0.6Na still exhibited the order–disorder transition of the ionic clusters, which was also shown in the thermal expansion studies (Figure 6). This fact indicates that some structural order remains in the fully hydrated ionic clusters. This result is interesting because a full amount of water could completely destroy the ordered arrangement within the ionic clusters. This will be discussed later.

General Discussion

Water Sorption Mechanism. This work reveals the behavior of water molecules sorbed in EMAA–sodium ionomers. The water molecules are incorporated into the COONa ion pairs in both the amorphous and ionic cluster regions with the following three stages: (1) at degrees of hydration lower than $y = 0.5$, water molecules are adsorbed at COONa ion pairs that are isolated in the amorphous region or are in the surface of the ionic clusters, showing Langmuir-type sorption behavior. (2) At the intermediate range of hydration from $y = 0.5$ to $y = 3$, the solution-type mechanism becomes predominant, where sorbed water molecules are absorbed into the inside of the ionic clusters and destroy some of the structural order. At $y = 3$, the primary hydration shell of the sodium ion is completed. Therefore, the number of water molecules forming the primary hydration shell in EMAA–0.9Na is 3 and smaller than the usual hydration number of 4 for the sodium ion. This is probably due to the weak acidity of the COOH groups. (3) At degrees of hydration higher than $y = 3$, a solution-type mechanism is still dominant, but water molecules are absorbed in the vicinity of the ionic clusters. We assume that these water molecules form an inverted micellar structure. The water molecules of more than three per COONa probably exist outside the primary hydration shell.

The sorbed water molecules in the hydrated EMAA–xNa ionomers also provide interesting dielectric phenomena. These results will be reported in a subsequent paper.

Structure of Ionic Clusters. Our DSC and dilatometric studies showed that the order–disorder transition still exists in the fully hydrated ionic clusters. Since the IR spectra indicate that the COONa ion pairs dissociate in the fully hydrated sample of EMAA–0.9Na as much as in the aqueous solution of sodium n-hexanoate, the remaining order within the fully hydrated ionic clusters may come from an orderness of the polyethylene chains incorporated into the ionic clusters. Therefore, we propose that the ionic clusters consist of two parts, the ordered assemblies of the COONa ion pairs and ordered polyethylene chains. As discussed in the section of the X-ray scattering results, we assume that reorganization of ionic clusters with hydration does not occur for carboxylated ionomers such as EMAA-based ionomers. Assuming that ΔH_i of the dry sample consists of ΔH_i(ion) and $\Delta H_i(CH_2)$, ΔH_i of the fully hydrated EMAA–0.9Na (about 8.6 J/g) would reflect that orderness of the polyethylene chains in

the ionic clusters. Since ΔH_i of the dry EMAA–0.9Na is about 25.8 J/g, we obtain 17.2 J/g as ΔH_i(ion). This is two-thirds of ΔH_i of the dry EMAA–0.9Na. The values of $\Delta H_i(CH_2)$ and ΔH_i(ion) of the dry EMAA–0.6Na are also calculated to be 6.6 and 14.8 J/g, respectively; the latter value is also about two-thirds of ΔH_i (21.4 J/g) of the dry EMAA–0.6Na.

Assuming the heat of fusion of polyethylene crystallites (4.01 kJ/mol of CH_2[42]) as the enthalpy change (J/mol of CH_2) of the polyethylene part, and that all COONa ion pairs are incorporated into the ionic clusters, the averaged numbers of CH_2 units per COONa group in the ionic clusters are calculated as 1.4 for EMAA–0.9Na and 1.6 for EMAA–0.6Na. Here, we should recognize that these values are a lower limit because of the approximations used here. Although we used a very rough estimation, we conclude that the ordered ionic clusters consist of the COONa ion pairs and a small portion of the polyethylene backbones.

Although our water sorption experiments give no direct information on the morphology of ionic clusters in ethylene ionomers, it is interesting to compare our order–disorder transition model with other morphological models for the ionic aggregates in ionomers, for example, the core–shell model,[22] the liquid-like model,[39,40] and the multiplet–cluster model.[43] Our model does not differ from the above three models in that ionic clusters contain hydrocarbon chains attached to and surrounding ionic assemblies, which is an easily accepted picture for the ionic clusters. Our model is, however, different in assuming that each ionic cluster consists of ordered assemblies of ion pairs and ordered CH_2 chain regions. This work and our previous results obtained prefer the existence of an order–disorder transition of the ionic clusters in EMAA-based ionomers. Further experimental work is necessary to obtain the final answer.

Acknowledgment. We wish to thank Mr. Hisaaki Hara of Du Pont-Mitsui Polychemicals Co. Ltd. for his helpful discussion. We also wish to thank the Instrument Center, Institute for Molecular Science (IMS), for assistance in obtaining the X-ray scattering data; we particularly appreciate the help of Dr. Hiroshi Kitagawa and Mr. Masahiro Sakai of IMS. We are indebted to Mr. Masaru Kato of Toagosei Chemical Industry Co. Ltd. for the TG/DTA analysis. S.K. wishes to acknowledge the support of the Ministry of Education, Science, and Culture (Grant-in-Aid for Scientific Research No. 03750645).

References and Notes

(1) Eisenberg, A. *Macromolecules* **1970**, *3*, 147.
(2) Holiday, L., Ed. *Ionic Polymers*; Applied Science: London, 1975.
(3) Eisenberg, A., King, M., Eds. *Ion-Containing Polymers, Polymer Physics*; Academic Press: New York, 1977; Vol. 2.
(4) Pineri, M., Eisenberg, A., Eds. *Structure and Properties of Ionomers*; NATO ASI Series C: Mathematical and Physical Sciences; D. Reidel Co.: Dordrecht, 1987; Vol. 198.
(5) Utracki, L. A., Weiss, R. A., Eds. *Multiphase Polymers: Blends and Ionomers*; ACS Symposium Series 395; American Chemical Society: Washington, DC, 1989.
(6) Eisenberg, A., Yeager, H. L., Eds. *Perfluroinated Ionomer Membranes*; ACS Symposium Series 180; American Chemical Society: Washington, DC, 1982.
(7) Yano, S.; Hirasawa, E.; Tadano, K.; Yamauchi, J.; Kamiya, Y. *Macromolecules* **1989**, *22*, 3186.
(8) Yano, S.; Tadano, K.; Hirasawa, E.; Yamauchi, J. *Macromolecules* **1990**, *23*, 4872.
(9) Longworth, R.; Vaughan, D. J. *Nature* **1968**, *218*, 85.
(10) Tadano, K.; Hirasawa, E.; Yamamoto, Y.; Yamamoto, H.; Yano, S. *Jpn. J. Appl. Phys.* **1987**, *26*, L1440.
(11) Tadano, K.; Hirasawa, E.; Yamamoto, H.; Yano, S. *Macromolecules* **1989**, *22*, 226.
(12) Yano, S.; Yamamoto, H.; Tadano, K.; Yamamoto, Y.; Hirasawa, E. *Polymer* **1987**, *28*, 1965.
(13) Yano, S.; Nagao, N.; Hattori, M.; Hirasawa, E.; Tadano, K. *Macromolecules* **1992**, *25*, 368.
(14) Hirasawa, E.; Yamamoto, Y.; Tadano, K.; Yano, S. *Macromolecules* **1989**, *22*, 2776.
(15) Hirasawa, E.; Yamamoto, Y.; Tadano, K.; Yano, S. *J. Appl. Polym. Sci.* **1991**, *42*, 351.
(16) Tsunashima, K.; Kutsumizu, S.; Hirasawa, E.; Yano, S. *Macromolecules* **1991**, *24*, 5910.
(17) Kutsumizu, S.; Hashimoto, Y.; Yano, S.; Hirasawa, E. *Macromolecules* **1991**, *24*, 2629.
(18) Hirasawa, E.; Hamazaki, H.; Tadano, K.; Yano, S. *J. Appl. Polym. Sci.* **1992**, *42*, 621.
(19) Hirasawa, E.; Tadano, K.; Yano, S. *J. Polym. Sci., Polym. Phys. Ed.* **1992**, *29*, 753.
(20) Marx, C. L.; Caulfield, D. F.; Cooper, S. L. *Macromolecules* **1973**, *6*, 344.
(21) Longworth, R. Reference 2, p 163.
(22) MacKnight, W. J.; Taggart, W. P.; Stein, R. S. *J. Polym. Sci., Polym. Symp.* **1974**, *45*, 113.
(23) Ishioka, T.; Kobayashi, M. *Macromolecules* **1990**, *23*, 3183.
(24) Read, B. E.; Carter, E. A.; Connor, T. M.; MacKnight, W. J. *Br. Polym. J.* **1969**, *1*, 123.
(25) Brozoski, B. A.; Painter, P. C.; Coleman, M. M. *Macromolecules* **1984**, *17*, 1591.
(26) Han, K.; Williams, H. L. *J. Appl. Polym. Sci.* **1991**, *42*, 1845.
(27) Itoh, K.; Tsujita, Y.; Takizawa, A.; Kinoshita, T. *J. Appl. Polym. Sci.* **1986**, *32*, 3335.
(28) Brozoski, B. A.; Coleman, M. M.; Painter, P. C. *Macromolecules* **1984**, *17*, 230.
(29) Lee, J. Y.; Painter, P. C.; Coleman, M. M. *Macromolecules* **1988**, *21*, 346.
(30) Umemura, J.; Cameron, D. G.; Mantsch, H. H. *J. Phys. Chem.* **1980**, *84*, 2272.
(31) Lowry, S. R.; Mauritz, K. A. *J. Am. Chem. Soc.* **1980**, *102*, 4665.
(32) Maeda, M.; Ohtaki, H. *Bull. Chem. Soc. Jpn.* **1975**, *48*, 3755.
(33) Falk, M. *Can. J. Chem.* **1980**, *58*, 1495.
(34) Eisenberg, D.; Kauzmann, W. *The Structure and Properties of Water*; Clarendon Press: London, 1969.
(35) Glew, D. N.; Rath, N. S. *Can. J. Chem.* **1971**, *49*, 837.
(36) Yasuda, M.; Tsujita, Y.; Takizawa, A.; Kinoshita, T. *Kobunshi Ronbunshu* **1989**, *46*, 347.
(37) Gierke, T. D.; Munn, G. E.; Wilson, F. C. *J. Polym. Sci., Polym. Phys. Ed.* **1981**, *19*, 1687.
(38) Roche, E. J.; Pineri, M.; Duplessix, R. *J. Polym. Sci., Polym. Phys. Ed.* **1982**, *20*, 107.
(39) Yarusso, D. J.; Cooper, S. L. *Polymer* **1985**, *26*, 371.
(40) Yarusso, D. J.; Cooper, S. L. *Macromolecules* **1983**, *16*, 1871.
(41) Tsatsas, A. T.; Reed, J. W.; Risen, W. M., Jr. *J. Chem. Phys.* **1971**, *55*, 3260.
(42) Brandrup, J.; Immergut, E. H.; McDowell, W. *Polymer Handbook*, 2nd ed.; John Wiley & Sons: New York, 1975.
(43) Eisenburg, A.; Hird, B.; Moore, R. B. *Macromolecules* **1990**, *23*, 4098.

Registry No. H_2O, 7732-18-5; ACR 1560 sodium salt, 25608-26-8.